Wear xxx (xxxx) xxx

Contents lists available at ScienceDirect

Wear

journal homepage: http://www.elsevier.com/locate/wear

Temperature compensation strategy for ultrasonic-based measurement of oil film thickness

Yaping Jia [a], Tonghai Wu [a,b,*], Pan Dou [a], Min Yu [c]

[a] Key Laboratory of Education Ministry for Modern Design and Rotor-Bearing System, Xi'an Jiaotong University, Xi'an, Shaanxi, 710049, PR China
[b] Xi'an Jinghui Information Technology Co., Ltd, PR China
[c] Department of Mechanical Engineering, Imperial College London, London, SW7 2AZ, United Kingdom

ARTICLE INFO

Keywords:
Ultrasonic measurement
Oil film thickness
Temperature compensation

ABSTRACT

Due to non-destructive testing characteristics, ultrasonic-based measurements are regarded as potential strategies in real-time monitoring of varied lubricant film thickness for tribological systems. Different theoretical models have been recently developed to calculate the film thickness from ultrasonic echo waves. However, the temperature influence on ultrasonic systems (for example, the acoustic parameters of materials and piezoelectric elements), which is non-negligible in the continuously running equipment, especially for heavy-loaded lubricated systems, has scarcely been considered. In this paper, the sensitivity of different parameters to the temperature variation is investigated in classical ultrasonic models. With the theoretical error analysis, a comprehensive temperature compensation strategy that considering the acoustic speed, material density, and reference signal, is proposed and integrated into the ultrasonic measurement algorithms. It is worth noting that the amplitude attenuation, waveform expansion, and signal time shift are considered in the compensation of the reference signal. Experimental verification is finally carried out in a calibrated rig with swept lubricant film thickness and different ambient temperatures. Test results suggest that the ultrasonic measurements with the proposed strategy effectively compensates the temperature influence and enables accurate calculations of lubricant film thickness under varying temperatures.

1. Introduction

The oil film thickness is a critical parameter to characterize the lubrication behaviour of mechanical equipment. Oil film with insufficient thickness will intensify the friction, wear, and even accelerate the failure of machine parts, while an overmuch thick oil film might cause enormous viscous dissipation [1]. Therefore, the examination of the oil film thickness is significant for machine condition monitoring, whereby proper lubrication control maintenance can be implemented timely to postpone or avoid oil film failure. Ultrasonic-based measurement, given its advantages of non-destructive detection, has been widely employed in industrial applications. Recently, a variety of computation models has been reported to extract thickness from echo signals for ultrasonic measurement. However, Further engineering applications are still frequently hindered. Specifically, the measurement under varying temperatures, which is common for most long-term running machines, is still challenging. As a result, efforts are still urgently needed to deploy this promising technique for real-time monitoring.

To calculate the film thickness from the reflection signals, different ultrasonic models have been proposed, including the time-of-flight method in time-domain [2] and the spring model, the resonance model, the phase model, the complex model in frequency-domain [3–9]. So far, ultrasonic models have been successfully applied on rolling bearing [10], sliding bearing [1,11], piston ring [12,13], seal [14,15] for lubricant film thickness. In addition, it is also used to explore the full film thickness profile, cavitation appearance, bearing deformation, seal failure, and piston secondary motion [10–15].

Within the current application of these ultrasonic models in real conditions, the temperature is recognized as an influential factor with respect to the measurement performance. Most of the critical parameters, including the acoustic speed, medium densities, and ultrasonic waves, are deeply associated with the temperature. Thereby the accuracy of the models is directly affected [1,10,13]. Such effects would be especially intensified during the monitoring of operating mechanical equipment where the temperature varies dramatically.

* Corresponding author. Key Laboratory of Education Ministry for Modern Design and Rotor-Bearing System, Xi'an Jiaotong University, Xi'an, Shaanxi, 710049, PR China.
E-mail address: wt-h@163.com (T. Wu).

https://doi.org/10.1016/j.wear.2021.203640
Received 19 September 2020; Accepted 13 December 2020
Available online 28 January 2021

Symbol

c_1	acoustic speed in the solid 1
c_2	acoustic speed in the oil layer
c_3	acoustic speed in the solid 2
z_1	acoustic impedance of the solid 1
z_2	acoustic impedance of the oil layer
z_3	acoustic impedance of the solid 2
ρ_2	oil density
R_{21}	reflection coefficient at the interface 1 (solid 1-oil) in the three-layered structure
R_{32}	reflection coefficient at the interface 2 (oil-solid 2) in the three-layered structure
f	signal frequency of the ultrasonic wave
f_c	central frequency of an ultrasonic transducer
f_m	resonance frequency the m-th mode
ω	angular frequency of the ultrasonic wave
h	oil film thickness
$\|R\|$	amplitude of reflection coefficient of the oil layer
Φ	phase of reflection coefficient of the oil layer
$\|R_K\|$	amplitude of reflection coefficient of the spring model
Φ_K	phase of reflection coefficient of the spring model
K	stiffness of the oil film
C	equivalent capacitance of the piezoelectric element
T	temperature
a	amplitude attenuation factor
b	waveform expansion factor
Δt	time shift factor
$x_T(t)$	reference signal at temperature T
$x_{T_0}(t)$	initial reference signal at temperature T_0
Δc	acoustic speed error
$\Delta\rho$	density error
Δz	acoustic impedance error
ΔR_{21}	error of the reflection coefficient at the interface 1
ΔR_{32}	error of the reflection coefficient at the interface 2
$\Delta\|R\|$	amplitude error of reflection coefficient of oil layer
$\Delta\Phi$	phase error of reflection coefficient of oil layer
$\Delta\|R_K\|$	amplitude error of reflection coefficient of the spring model
$\Delta\Phi_K$	phase error of reflection coefficient of the spring model
Δh	error of the calculated film thickness
$\Delta h/h$	relative error of the calculated film thickness

To accommodate this influence, scholars have carried out thermal calibration of acoustic speed by investigating the time difference of oil film reflection echo with known thickness at different temperatures [13]. For the compensation of the reference signal, Dwyer-Joyce and co-workers [16] collected and recorded multiple sets of reference signals in a specified temperature range to measure the oil film thickness of bearing with the spring model. The mathematical equation that can be used for reference signal amplitude compensation was obtained based on the numerical fitting method. This method has less computation, but the preliminary workload is massive. To get rid of the thermal calibration step, Reddyhoff and co-workers [15] proposed a self-compensation method by monitoring the amplitude of the "mediation echoes" such as the reflected echoes that reflected from the substrate-liner interface in a liner bearing. Based on the changes of this "mediation echoes" under temperature variations, the amplitude of the reference signal can be compensated with the same change ratio. However, for a typical three-layer structure, "mediation echoes" has to be obtained by modifying the structure geometry. Moreover, another concern over this method is that it requires two kinds of ultrasonic signals, echoes from the solid-solid interface and oil-solid interface, which will contaminate the results by involving more noise.

Currently, there are still some limitations regarding the temperature compensation of ultrasonic-based film thickness measurements. Firstly, systematic researches are scarcely reported on the temperature effects, the influence mechanism, the error evaluations, and the improvement of compensation factors. Secondly, the amplitude compensation is often accomplished within the spring model, while the phase compensation is rarely reported, which is the foundation of other models. Finally, the effects of the existing compensation methods have been rarely evaluated by calibrations, which may introduce uncertainties to the applications in various scenarios.

For this concern, a systematic study is carried out focusing on the effect of temperature on the ultrasonic-based measurement for lubricant film thickness. The temperature effect mechanism on those four models is investigated, and the measurement error is analyzed theoretically. Furthermore, the sensitive factors, including the acoustic speed, medium densities and reference signal are extracted. Thereby a comprehensive temperature compensation strategy is proposed. The proposed method is evaluated experimentally, and it is found that the comprehensive temperature compensation strategy considering the material parameters and reference signal can improve the accuracy of the ultrasonic models for oil film thickness calculation under variable temperatures.

The rest of this paper is organized as follows: Section 2 introduces the ultrasonic models and systematically analyzes the temperature effect. The single-factor compensation model and a comprehensive compensation strategy of oil film thickness are described in Section 3. The test rig and experimental results are presented in Section 4. Finally, the conclusions are drawn in Section 5.

2. Ultrasonic models and temperature effect

2.1. Ultrasonic models

To illustrate the principle of ultrasonic lubricant film measurement, a schematic of the typical three-layered sandwich structure (solid 1-lubricant- solid 2) is shown in Fig. 1. When the incident wave I is perpendicularly incident on the interface between the solid layer and the lubricant layer, portions of the signal are transmitted while others are reflected due to the acoustic impedance mismatch [9]. The echo reflected from the lubricant layer is denoted as $\{B_1, B_2, \ldots, B_n\}$. The proportion of reflected wave depends on the thickness of the layer and its acoustic properties.

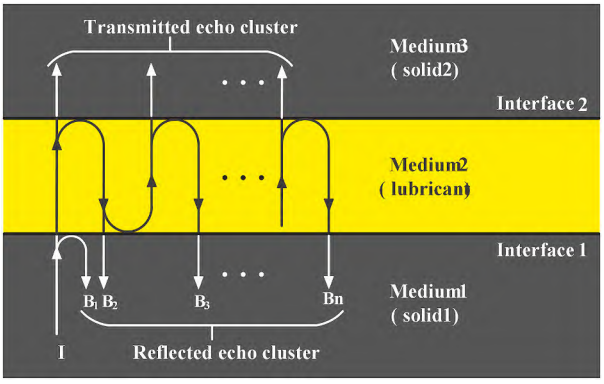

Fig. 1. Schematics of an ultrasonic wave traveling through a three-layered system.

The ultrasonic reflection coefficient is defined as the ratio of the reflected wave to the incident wave in the frequency-domain. As it is difficult to practically extract the incident signal, and the amplitude and the phase of the reflection coefficient at a solid to air boundary are approximately 1 and 0. Thus, the reflected signal from the stationary solid-air interface is used as an incident signal (namely reference signal). The amplitude and phase of the reflection coefficient [9] of the lubricant layer can be obtained by,

$$|R| = \left[\frac{(R_{21} + R_{32}\exp(-2\beta h))^2 - 4R_{32}R_{21}\exp(-2\beta h)\sin^2(2\pi f h/c_2)}{(1 + R_{32}R_{21}\exp(-2\beta h))^2 - 4R_{32}R_{21}\exp(-2\beta h)\sin^2(2\pi f h/c_2)}\right]^{1/2}, \tag{1}$$

$$\Phi = \tan^{-1}\left[\frac{R_{32}\exp(-2\beta h)(1 - R_{21}^2)\sin(4\pi f h/c_2)}{R_{21} + R_{32}\exp(-2\beta h)(1 + R_{21}^2)\cos(4\pi f h/c_2) + R_{21}R_{32}^2\exp(-4\beta h)}\right], \tag{2}$$

where R_{21} and R_{32} are the displacement reflection coefficients at interfaces 1 and 2, respectively, as shown in Fig. 1; β is the attenuation coefficient; f is the frequency of the ultrasonic wave; h is the lubricant film thickness. Reflection coefficients R_{21} and R_{32} can be further expressed as

$$R_{21} = \frac{z_2 - z_1}{z_2 + z_1}, R_{32} = \frac{z_3 - z_2}{z_3 + z_2} \tag{3}$$

where $z_i = \rho_i c_i$; z_i, ρ_i and c_i is the acoustic impedance, the density and the acoustic speed of medium $i (i = 1, 2, 3)$, as shown in Fig. 1.

According to the acoustic values of materials listed in Table 1, the relationship of the amplitude or phase of the reflection coefficient and the product of frequency and film thickness is calculated based on ignoring the attenuation factor, as shown in Fig. 2.

When the thickness of the lubricant layer is less than the wavelength of the ultrasonic wave, the reflection coefficient depends on the stiffness of the lubricant K. The amplitude of the reflection coefficient $|R_K|$ and the phase of the reflection coefficient Φ_K of the stiffness-controlled zone, that is, the spring model zone, is expressed as [17,18]:

$$|R_K| = \sqrt{\frac{(\omega z_1 z_3)^2 + K^2(z_3 - z_1)^2}{(\omega z_1 z_3)^2 + K^2(z_3 + z_1)^2}}, \tag{4}$$

$$\Phi_K = \arctan\left(\frac{2\omega z_1 z_3^2/K}{(z_3 - z_1) + \omega^2(z_1 z_3/K)^2}\right), \tag{5}$$

where $K\left(=\frac{\rho_2 c_2^2}{h}\right)$ is the stiffness of the lubricant film; ω is the angular frequency of the ultrasonic wave.

If $z_1 = z_3 = z$, the film thickness in the spring model zone can be calculated with the amplitude of the reflection coefficient and the acoustic values of materials by

$$h = \frac{2\rho_2 c_2^2}{\omega z}\sqrt{\frac{|R_K|^2}{1 - |R_K|^2}}, \tag{6}$$

or with the phase of the reflection coefficient and the acoustic values of materials by

$$h = \frac{2\rho_2 c_2^2}{\omega z \tan\Phi_K}. \tag{7}$$

Table 1
Acoustic properties of different materials in three-layered structures.

Material	Density ($kg \cdot m^{-3}$)	Acoustic speed ($m \cdot s^{-1}$)	Acoustic impedance (10^6 kg m^{-2} s^{-1})
oil	886	1467	1.30
steel	7810	5818	45.4

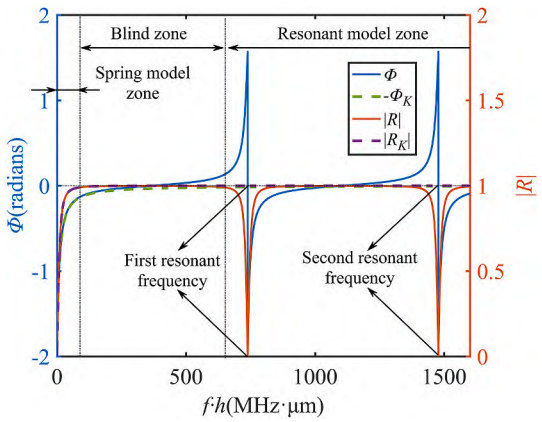

Fig. 2. Variation of the amplitude or phase of the reflection coefficient with the product of frequency and thickness [9].

When the film thickness is an integer multiple of half-wavelength of the ultrasonic wave, a series of minimum points appear periodically in the amplitude spectrum of the reflection coefficient. Correspondingly, a series of zero-crossing points can be found in the phase spectrum of the reflection coefficient. The frequencies corresponding to these minimum points or zero-crossing points are the resonance frequencies. With the acoustic speed, the film thickness in the resonance model zone can be calculated by Ref. [17]:

$$h = \frac{c_2 m}{2 f_m}, \tag{8}$$

where m is the resonant order, and f_m is the resonant frequency.

When the film thickness is in the blind zone, the film thickness has a one-to-one mapping relationship with the phase of the reflection coefficient, as indicated in Fig. 2. Therefore, the film thickness can be solved iteratively, according to the phase model given in Eq. (2).

The spring model, the resonance model, and the phase model all take the amplitude or phase information of the reflection coefficient to calculate the film thickness respectively, while simultaneously employing the amplitude and phase information of the reflection coefficient can also obtain the film thickness by Ref. [8]:

$$h = \frac{c_2}{4\pi f}\tan^{-1}\left(\frac{|R|\sin\Phi(1 - R_{21}^2)}{-R_{21} - |R|^2 \cdot R_{21} + |R|\cos\Phi + |R|\cos\Phi \cdot R_{21}^2}\right) \tag{9}$$

2.2. Temperature effect on ultrasound model

Regarding the above ultrasonic models, the effect of temperature includes two parts: the effect on the material properties of the lubricant and the solid; and the effect on piezoelectric elements.

2.2.1. Effect of temperature on lubricant and solid

Essentially, an increasing temperature will lead to the change of density and elastic modulus, and then affects the ultrasonic propagation velocity, acoustic impedance, and interface reflection coefficient.

On the other hand, considering the thermal expansion and contraction effect of the material, the solids would expand with the increasing temperature, therefore change the propagation distance of ultrasonic waves. Thereby, the propagation time would change consequently. The above changes could be reflected by the overall time shift of the ultrasonic waveform.

2.2.2. Effect of temperature on piezoelectric elements

The piezoelectric element can be regarded as a capacitor with opposite charges on two plates, and its equivalent capacitance C is

$$C = \frac{eA}{d}, \tag{10}$$

where e is the dielectric constant; A is the polarization area; d is the thickness of the piezoelectric element.

Intrinsically, there is a strong correlation between the dielectric constant and the temperature. Therefore, the change of dielectric constant caused by the varying temperature would induce the change of equivalent capacitance. The effects of temperature can be discussed as follows.

1) Change the amplitude of the signal

The relationship between the output of the piezoelectric element V_{out} and its equivalent capacitance C is as follows:

$$V_{out} = \frac{Q_z}{C}, \tag{11}$$

where Q_z is the amount of charge on the surface of the piezoelectric sheet.

As a result, the change of equivalent capacitance caused by temperature change the output voltage of piezoelectric components. Thus the amplitude of the signal from the piezoelectric element would be changed correspondingly.

2) Change the waveform of the signal

Due to the limitation of the effective bandwidth of different piezoelectric elements, the range of oil film thickness may not be fully explored by one sensor with a fixed central frequency. To address this, Dwyer-Joyce and co-workers [19] proposed a design of piezoelectric elements based on the LC circuit, which can adjust the central frequency and effective bandwidth by changing the inductance value:

$$f_c = \frac{1}{2\pi\sqrt{LC}}, \tag{12}$$

where f_c is the central frequency; L is the inductance value, and C is the equivalent capacitance of the piezoelectric element.

The hollow inductance does not change with the temperature, and the core inductance changes only when the temperature reaches Curie temperature. The change of equivalent capacitance caused by temperature will change the central frequency and effective bandwidth of piezoelectric components in frequency-domain. This phenomenon can be described as the stretching of the signal waveform in time-domain, considering the time-stretching property of the fast Fourier transform (FFT).

In conclusion, the acoustic properties of materials and the reference signal will change under variable temperatures for ultrasonic-based measurement of oil film thickness.

2.3. Error analysis

Follow the analysis in Section 2.2, it is confirmed that temperature affects the acoustic properties of materials and the reference signal. To identify the variables need temperature compensation, error analysis is carried out in this section.

For the film thickness measurement model based on ultrasound, the errors caused by temperature is shown in Fig. 3, where Δc and $\Delta\rho$ are the errors of acoustic speed and density caused by temperature change; and Δz, ΔR_{21}, and ΔR_{32} are the errors of acoustic impedance and interface reflection coefficient caused by acoustic speed and density; $\Delta|R|$ and $\Delta\Phi$ are the errors of the amplitude and phase of the reflection coefficient introduced by the time shift, waveform expansion, and amplitude attenuation of the reference signal; Δh is the final calculation error of film thickness caused by the temperature variation.

2.3.1. Error analysis of acoustic properties of materials

The acoustic speed and density are regarded as independent variables, and the coupling effects on acoustic impedance and the interface reflection coefficient are considered. According to the relationship between the material properties and the temperature T shown in Table 2, the relative error of calculated thickness $\Delta h/h_0$ introduced by the

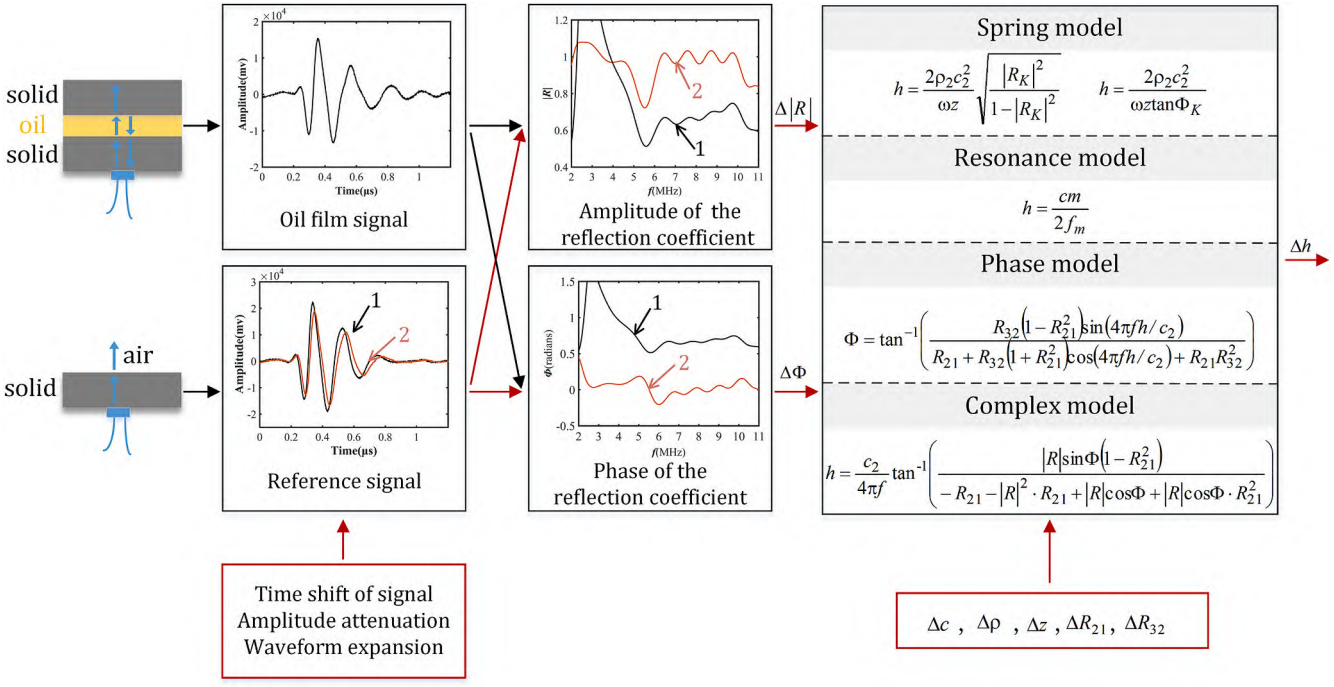

Fig. 3. Illustration of temperature affects the ultrasonic measurement of oil film thickness. The reference signal 1 represents the reference signal at room temperature (namely initial reference signal), and the reference signal 2 represents the reference signal affected by temperature, and the amplitude and phase of the reflection coefficient correspond respectively.

Table 2
Properties of materials.

Material	Density (kg·m^{-3})	Acoustic speed (m·s^{-1})
Oil[a]	$\rho = 888/(1 + 0.0007(T - 20))$	$c = 0.0039T^2 - 3.39T + 1555.2$
Steel[b]	$\rho = 7955/(1 + 3\alpha(T + 273))$	$c = 5244 \times 10^3(1 - 11\alpha(T + 273))$

[a] High-performance marine diesel engine mineral oil.
[b] GH128.

influence of temperature on an independent variable is also given, where the calculated thickness h_0 at 20 °C is taken as a reference.

For different calculated thickness h_0, relative errors of the calculated thickness $\Delta h/h_0$ of the spring model and the resonance model are identical at the same temperature. Therefore, the relative error of the calculated thickness with acoustic speed and density affected by the varying temperature is simplified, as shown in Fig. 4.

The relative error of the calculated film thickness of the phase model introduced by independent variables is shown in Fig. 5. It can be seen that the acoustic parameters of the oil have a greater influence on the calculation results of film thickness than steel.

The relative error of the calculated thickness of the complex model is shown in Fig. 6. It can be observed that the impact of steel can be ignored.

It can be observed that for each ultrasonic model, the change of acoustic speed and density of oil has non-negligible effects on the calculation result of film thickness, while the impact of steel can be ignored. Therefore, it is necessary to compensate for the acoustic parameters of oil.

2.3.2. Error analysis of the reference signal

The change of the reference signal caused by the temperature will result in the improper acquisition of the amplitude and phase of the reflection coefficient. The spring model, the phase model, and the complex model are highly dependent on the accurate amplitude and phase of the reflection coefficient. Assuming that there is an error $\Delta|R|$ or $\Delta|R_K|$ disturbing the amplitude of the reflection coefficient and an error $\Delta\Phi$ or $\Delta\Phi_K$ in the phase of the reflection coefficient, the relative error of the calculated thickness $\Delta h/h$ can be derived in Table 3.

For each model, the relative errors of the calculated thickness introduced by the amplitude or the phase of the reflection coefficient are plotted in Fig. 7 (a), (b), (c), and (d), respectively. It can be observed that small errors in the amplitude or phase of the reflection coefficient may lead to significant relative errors in calculated thickness. Therefore, the compensation of the reference signal is a pivotal factor in maintaining the accuracy of the film thickness measurement.

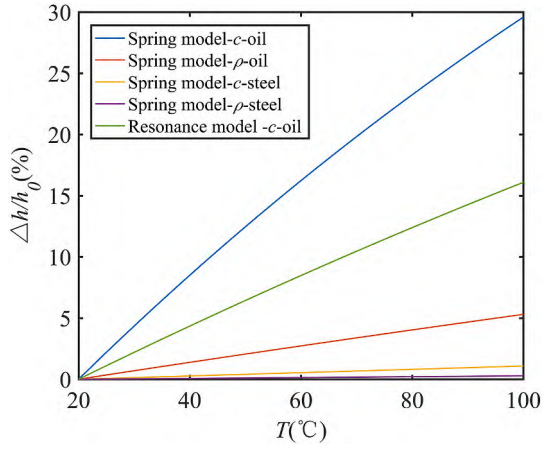

Fig. 4. The relative error of the calculated thickness of the spring model and the resonance model with acoustic speed and density affected by temperature.

3. Temperature compensation strategy

The analysis in section 2.3 suggests that the acoustic speed of oil, the density of oil, and the reference signal are three crucial factors to guarantee the accuracy of the film thickness measurement. Therefore, corresponding compensation models for each factor are established, respectively, and a comprehensive temperature compensation strategy for the ultrasonic-based measurement of oil film thickness is proposed in this section.

3.1. The compensation of acoustic speed

For the thick layer, the time interval of the reflected echoes from the oil layers can be directly extracted in time-domain for the calculation of the acoustic speed as:

$$c_2 = \frac{2h}{t_s}, \tag{13}$$

where c_2 is the acoustic speed; t_s is the time interval of the reflected echoes; h is the thickness of the oil layer. According to the acoustic speed calculated at different temperatures, a mathematical relationship can be obtained to compensate for the acoustic speed, based on the numerical fitting method.

3.2. The compensation of density

For the compensation of lubricants, Dowson and Higginson proposed a density formula considering thermal effect as

$$\rho_T = \rho_0[1 + C_1 p / (1 + C_2 p) - C_3(T - T_0)], \tag{14}$$

where ρ_T is the density at T, ρ_0 is the density at T_0, C_1 and C_2 are the density-pressure coefficient, $C_1 = 0.6 \times 10^{-9} Pa^{-1}$, $C_2 = 1.7 \times 10^{-9} Pa^{-1}$, C_3 is the density-temperature coefficient, $C_3 = 0.00065 K^{-1}$.

3.3. The compensation of reference signal

Given the analysis in Section 2.2, it is obvious that the influence of temperature on the time-domain reference signal can be summarized as time shift, amplitude attenuation, and waveform expansion. However, the amplitude compensation is accomplished within the spring model, while the phase compensation is not involved, which is the foundation of other models. Therefore, a time-domain reference signal compensation model that comprehensively considers the signal time shift, amplitude attenuation, and waveform expansion is proposed in this paper. The reference signal at the actual temperature, $x_T(t)$, is obtained by compensating the reference signal at the initial temperature $x_{T_0}(t)$ via

$$x_T(t) = a \cdot x_{T_0}\left(\frac{1}{b}t - \Delta t\right), \tag{15}$$

where a is the amplitude attenuation factor, b is the waveform expansion factor, and Δt is the time shift factor.

To obtain the amplitude attenuation factor and the waveform expansion factor, thermal calibration is needed and further details are given as follows.

- The oil film in the three-layered structure is removed, the reflected signal from the "solid-air" structure at environmental temperature is then taken as the initial reference signal.
- The "solid-air" structure is heated, and a series of reference signals at different temperatures are collected.
- The amplitude attenuation factor and wave expansion factor at different temperatures are calculated. It is worth noting that the amplitude attenuation factor is defined as the ratio of the maximum or minimum amplitude of the reference signal at different

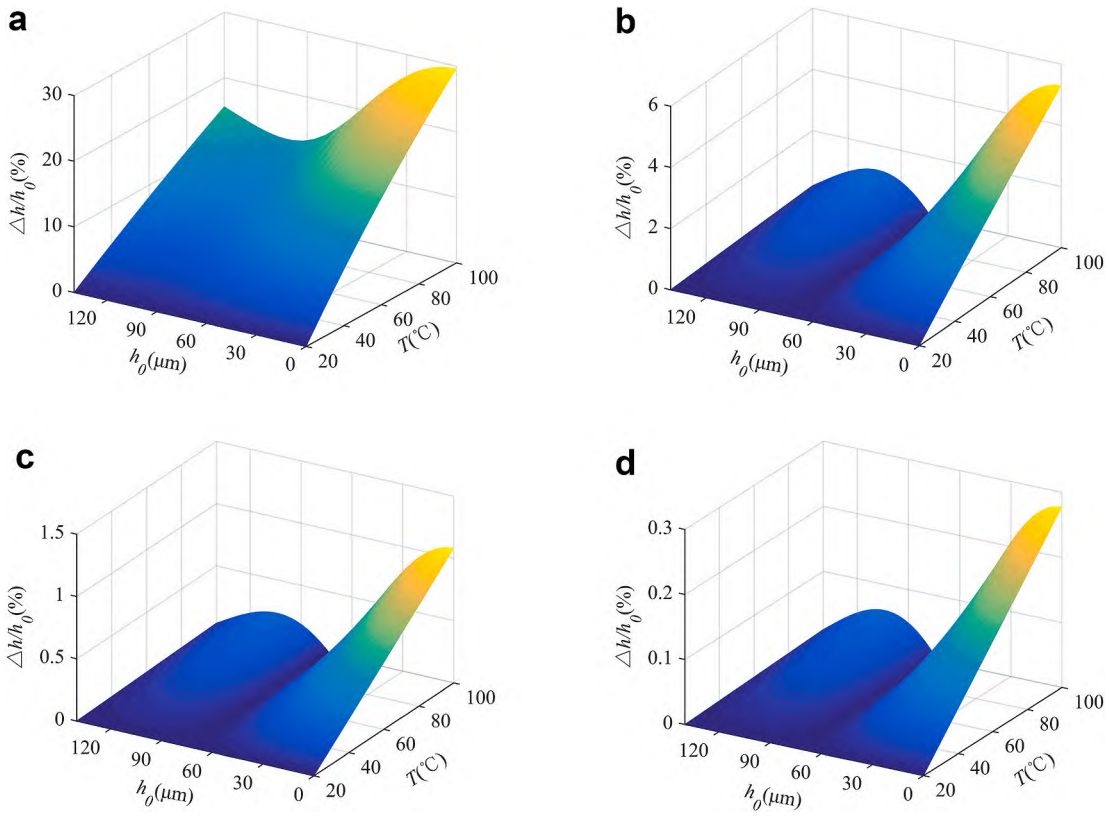

Fig. 5. The relative error of the calculated thickness of the phase model introduced by (a) acoustic speed of oil, (b) density of oil, (c) acoustic speed of steel, and(d) density of steel. The central frequency of the ultrasonic transducer is 5 MHz.

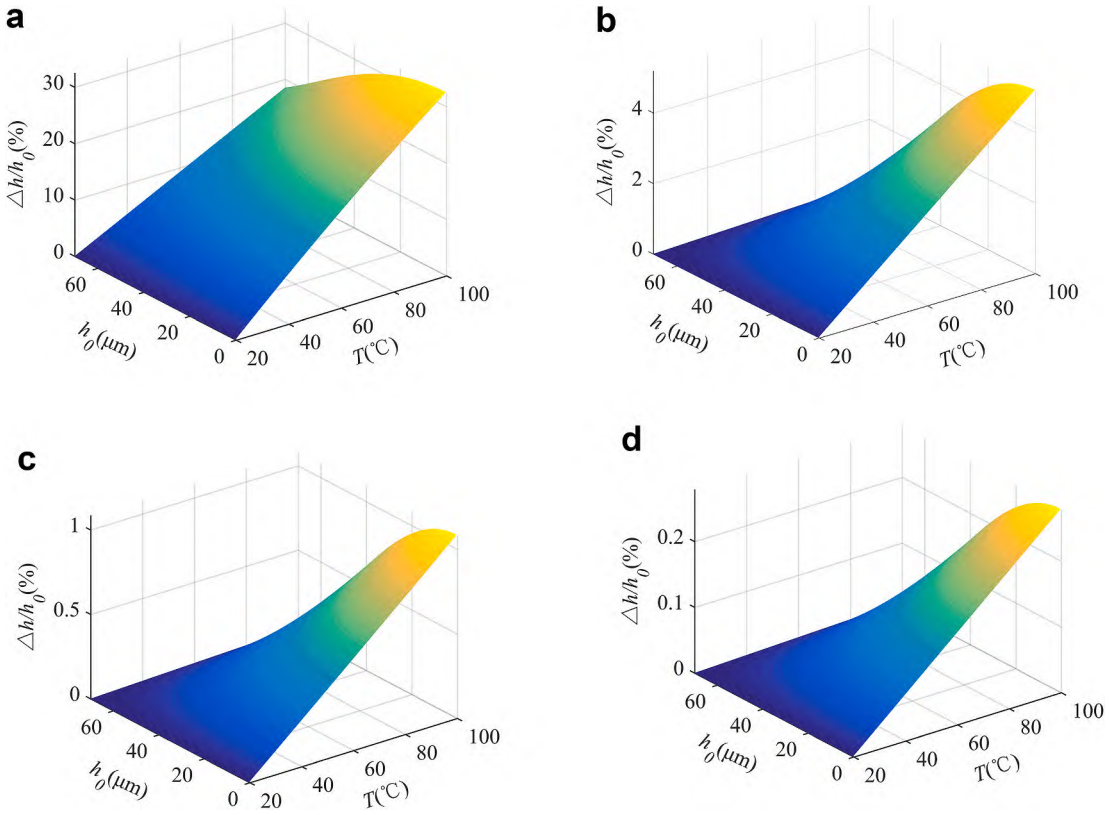

Fig. 6. The relative error of the calculated thickness of the complex model introduced by (a) acoustic speed of oil, (b) density of oil, (c) acoustic speed of steel, and (d) density of steel. The central frequency of the ultrasonic transducer is 5 MHz.

Table 3
The relative error of the calculated thickness.

Model	Relative error of the calculated thickness $\Delta h/h$
Spring model - amplitude	$\frac{\Delta h}{h}=\frac{\partial h}{\partial\lvert R_K\rvert}\times\frac{\Delta\lvert R_K\rvert}{h}=\frac{\Delta\lvert R_K\rvert}{\lvert R_K\rvert-\lvert R_K\rvert^3}$
Spring model - phase	$\frac{\Delta h}{h}=\frac{\partial h}{\partial\Phi_K}\times\frac{\Delta\Phi_K}{h}=-\Delta\Phi_K\frac{(\tan\Phi_K)^2+1}{\tan\Phi_K}$
Phase model [8]	$\frac{\Delta h}{h}=\frac{\partial h}{\partial\Phi}\times\frac{\Delta\Phi}{h}=\frac{1}{\frac{\partial\Phi}{\partial h}}\times\frac{\Delta\Phi}{h}$
Complex model [8]	$\frac{\Delta h}{h}=\frac{\sqrt{\left\lvert\frac{\partial h}{\partial\lvert R\rvert}\times\Delta\lvert R\rvert\right\rvert^2+\left\lvert\frac{\partial h}{\partial\Phi}\times\Delta\Phi\right\rvert^2}}{h}$

temperatures to the initial reference signal in the time domain. To reduce the error, the average is taken as the final amplitude attenuation factor. The waveform expansion factor is defined as the ratio of the time interval between two maximum amplitude of the reference signal at different temperatures to the initial reference signal in the time domain.

- The mathematical equations of amplitude attenuation factor and waveform expansion factor with temperature are obtained by the numerical fitting.
- In the process of film thickness measurement, the amplitude attenuation factor and the waveform expansion factor at the actual temperature are obtained by the above mathematical equations.

To obtain the time shift factor, a self-compensation method is proposed. For the three-layer structure, as shown in Fig. 1, it is assumed that the time-domain expression of the reference signal is $X(t)$. According to the wave superposition principle, the time-domain expression of the oil film signal $Y(t)$ [20] is

$$Y(t)=V_{12}X(t)+W_{12}V_{23}W_{21}X(t-2t_i)+W_{12}V_{23}W_{21}(V_{12}V_{23})^1X(t-4t_i)+\cdots+W_{12}V_{23}W_{21}(V_{12}V_{23})^{n-2}X(t-2(n-1)t_i), \tag{16}$$

where t_i is the flight time interval of ultrasonic at the oil layer; W_{ij} and $V_{ij}(i,j=1,2,3)$ are the transmission coefficients and reflection coefficients at the interfaces of media i and j in Fig. 1, respectively. W_{ij} and V_{ij} can be further expressed as

$$V_{ij}=\frac{z_i-z_j}{z_i+z_j},V_{ji}=-V_{ij},W_{ij}=1+V_{ij},W_{ji}=1-V_{ij}, \tag{17}$$

where z_i and z_j are the acoustic impedance of medium i and j, respectively.

Ultrasonic pulse has bandwidth characteristic, and the time domain form of the reference signal can be simulated by Gaussian echo $I(t)$ [21,22]:

$$I(t)=\beta e^{-\alpha(t-\tau)^2}\cos(2\pi f_c(t-\tau)+\phi), \tag{18}$$

where β is the amplitude; α is the bandwidth factor; τ is the arrival time; f_c is the central frequency; ϕ is the phase.

Fig. 8 shows the reference signal simulated by the Gaussian echo and the oil film signals of different thicknesses obtained as Eq. (16), Eq. (19) and the material acoustic parameters shown in Table 1. Among them, the reference signal is [20].

$$X(t)=-2091e^{-92.4(t-0.4)^2}\cos(13.6\pi(t-0.4)+4.5). \tag{19}$$

It can be seen that the reference signal and the oil film signal share the same starting point P in the time domain. This is because the

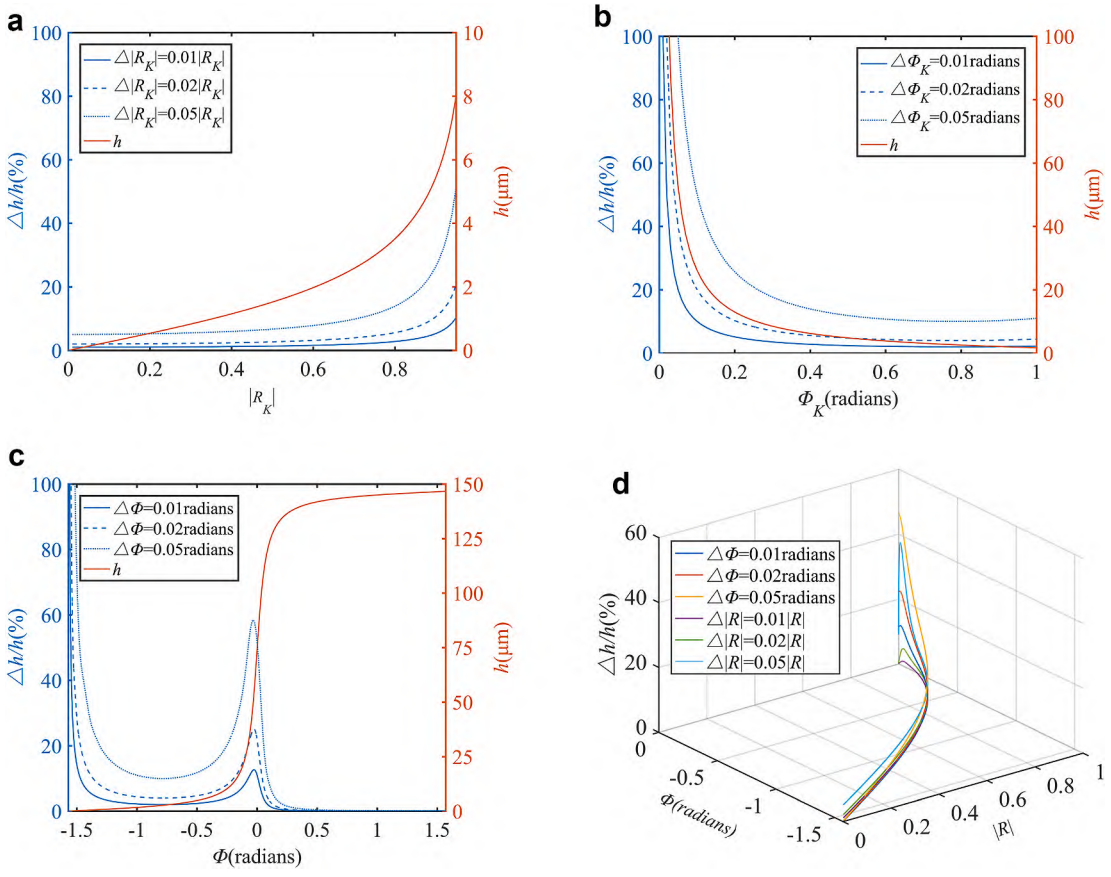

Fig. 7. The relative error of the calculated thickness introduced by the reflection coefficient amplitude or phase for (a) spring model – amplitude, (b) spring model – phase, (c) phase model, (d) complex model. The central frequency of the ultrasonic transducer is 5 MHz.

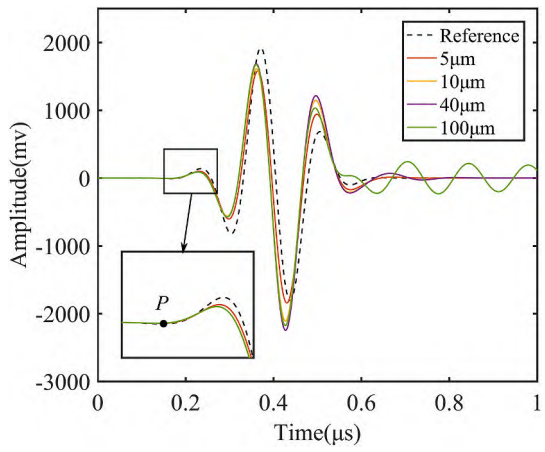

Fig. 8. The reference signal and oil film signal simulated by Gaussian echo.

reference signal propagates over a same distance as the oil film reflected echo B_1, as shown in Fig. 1. Although the echo $\{B_2, B_3, \cdots, B_n\}$ will counteract the echo B_1 somehow, it will not completely eliminate the reflected echo B_1. Therefore, the time shift factor can be obtained by aligning the starting point P of the initial reference signal with the oil film signal in the time domain during the film thickness measurement.

In oil film thickness measurement, the acoustic speed and density values at the actual temperature are obtained according to the relationship between the acoustic speed, density, and temperature. The actual reflection coefficient amplitude and phase are measured according to the oil film signal and the compensated reference signal. These values are used in each ultrasonic measurement model to achieve accurate measurement of the oil film thickness.

4. Experimental validation

In this section, the proposed reference signal compensation model considering the signal time shift, amplitude attenuation, and waveform expansion is verified. Then further validation of the comprehensive temperature compensation strategy for the ultrasonic-based measurement of oil film thickness proposed in this paper is conducted, which considering the acoustic speed, density, and reference signal.

4.1. Experimental apparatus

The experiment apparatus is similar to those reported in the literature [6,9], which consists of two components, a positioning rig, and an ultrasonic measurement system, as shown in Fig. 9. The positioning rig is configured to accurately control the oil film thickness, which consists of a stationary disk, a movable disk, and a micrometer. The ultrasonic measurement system includes an ultrasonic piezoelectric element, an ultrasonic pulser-receiver system, a digitizing card, and a personal computer to transmit, collect, and process ultrasonic signals. The piezoelectric element was bonded to the back face of the stationary steel disk, and its central frequency is 5.4 MHz.

4.2. Compensation experiment of reference signal

The material properties of the three-layer structure (steel-oil-steel) used in the experiment are shown in Table 1. The reflected signal of the steel-air interface is taken as the reference signal. The positioning rig was heated in the temperature control box, and the temperature is measured by a thermocouple. The original time-domain data of the reference signal were captured in the range of 30 ~ 80 °C with a temperature interval of 2 °C, as shown in Fig. 10. It can be observed that with the increase of temperature, the reference signal indicates the changes of time shift, amplitude attenuation, and waveform expansion, which is consistent with the theoretical analysis in Section 2.2.

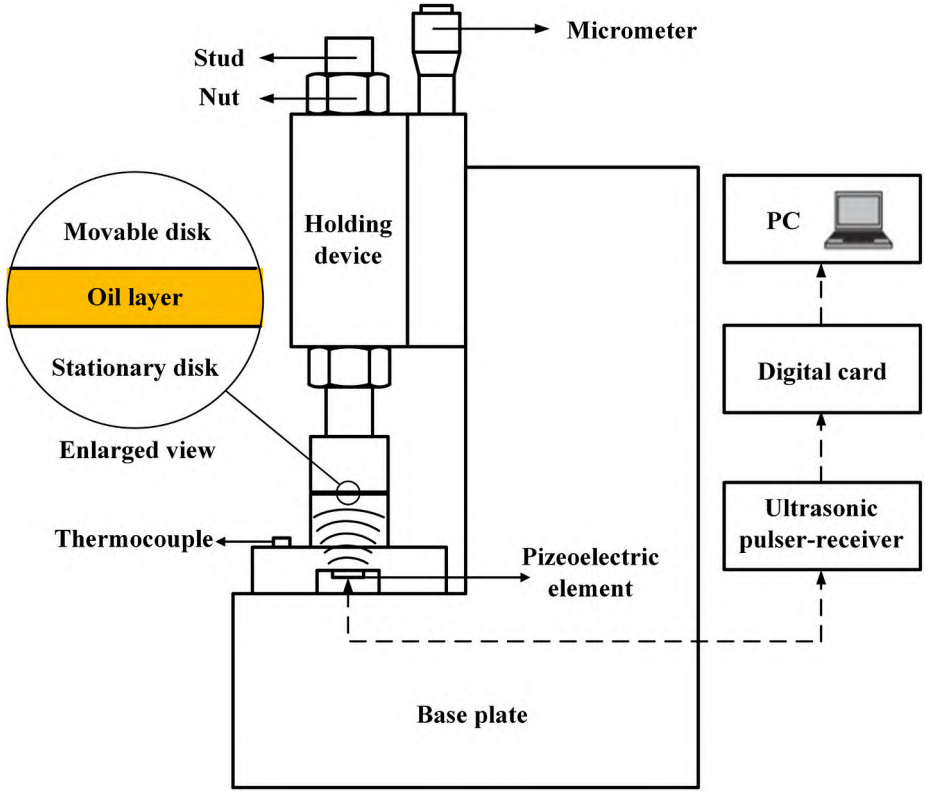

Fig. 9. The experimental facility for controlling and measuring oil film thickness between two solid layers [6,9].

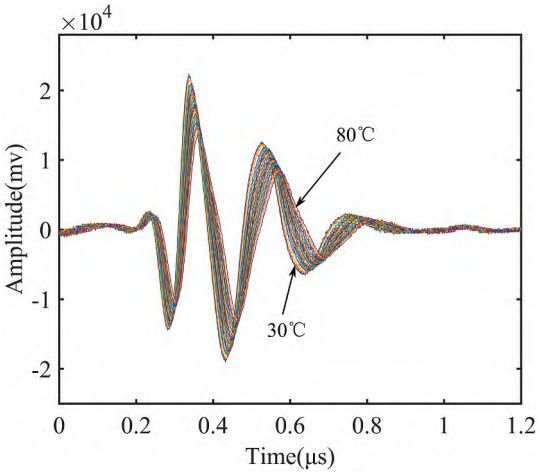

Fig. 10. The original time-domain data of the reference signal collected in the range of 30 ~ 80 °C and the temperature interval is 2 °C.

The amplitude attenuation factor and the waveform expansion factor of the reference signal at different temperatures relative to the initial reference signal are shown in Fig. 11. The reference signal at 30 °C is taken as the initial reference signal. For subsequent verification, only part of the data is selected. Based on the method of numerical fitting, the equations of amplitude attenuation factor and waveform expansion factor varying with temperature are obtained. It can be seen that the amplitude attenuation factor and waveform expansion factor have an excellent linear relationship with temperature.

To verify the effectiveness of the method, the comprehensive compensation model proposed in this paper is used to compensate the initial reference signal and compared with the measured signal at actual temperature (namely actual reference signal). The amplitude attenuation factor and the waveform expansion factor were calculated via the equations of amplitude attenuation factor and waveform expansion factor varying with temperature. The time shift factor was obtained by aligning the starting point *P* of the initial reference signal and oil film signal at different temperatures, as shown in Fig. 8.

The initial reference signal at 30 °C, the compensated reference signal, and the actual reference signal at 50 °C are shown in Fig. 12. It can be seen that the compensated reference signal is highly consistent with the actual reference signal.

The amplitude spectrum and the phase spectrum of these signals were obtained using a fast Fourier transform (FFT) and the results are shown in Fig. 13. It can be observed that the compensation method of the reference signal has a reasonable compensation effect. Moreover, as shown in Fig. 13 (a), due to the amplitude attenuation and waveform expansion, the amplitude spectrum of the initial reference signal and the actual signal has errors. The phase spectrum of the initial reference signal and the actual signal has an enormous error due to the signal time shift and waveform expansion, as shown in Fig. 13 (b).

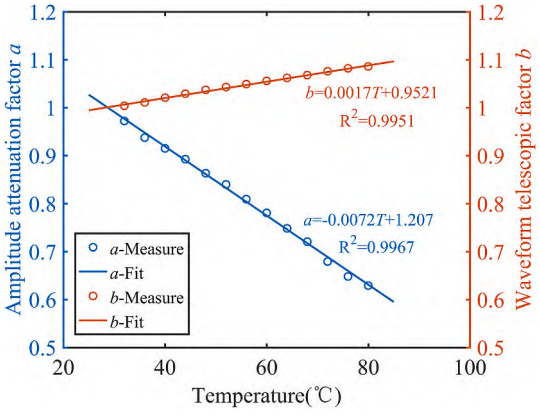

Fig. 11. The amplitude attenuation factor and waveform expansion factor of the reference signal at different temperatures relative to the initial reference signal. The initial reference signal is the reference signal at 30 °C.

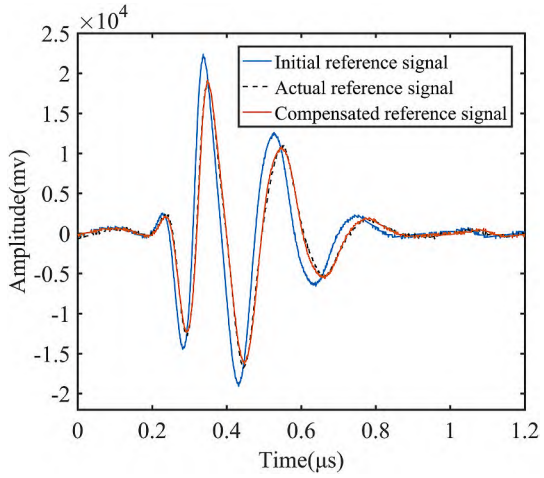

Fig. 12. The initial reference signal at 30 °C, the compensated reference signal and the actual reference signal at 50 °C in the time domain.

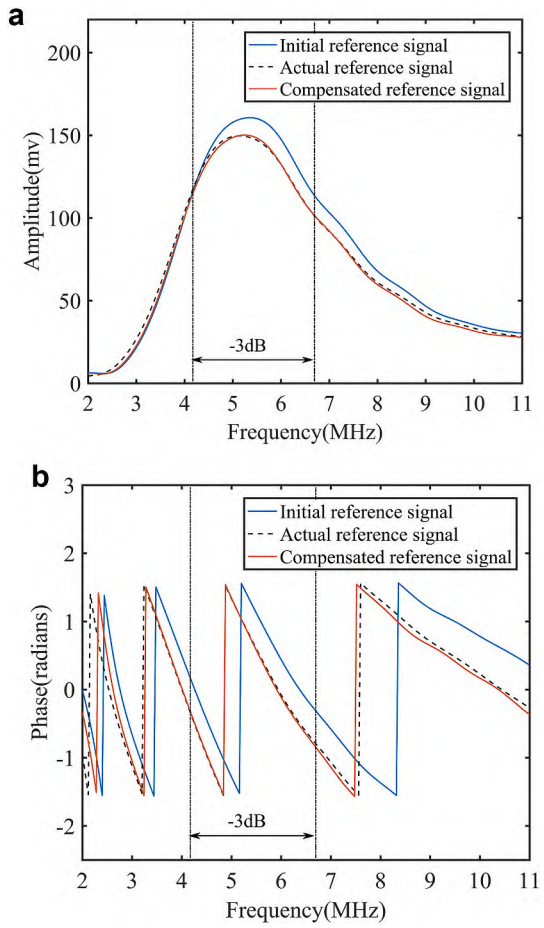

Fig. 13. The amplitude spectrum (a) and phase spectrum (b) of the initial reference signal (30 °C), the actual signal (50 °C), and the compensated reference signal (50 °C).

The relative error of the amplitude and the absolute error of the phase between the compensated reference signal and the uncompensated reference signal (that is the initial signal) and the actual reference signal are shown in Fig. 14 (a) and (b), respectively. It can be observed that the error of the reference signal obtained by the comprehensive compensation strategy proposed in this paper is trivial in the -3dB bandwidth (4.2–6.6 Mhz).

To reduce the noise interference, the average error within -3dB bandwidth is taken as the index of evaluating the compensation effect, and the same method is used to compensate the reference signal at other temperatures. The amplitude error of the compensation reference signal at different temperatures is shown in Fig. 15 (a), and the phase error is shown in Fig. 15 (b). It can be observed that the comprehensive compensation model proposed in this paper has a reasonable compensation effect, compared with the uncompensated reference signal. The maximum relative error of the amplitude is reduced to 3%, and the absolute phase error is less than 0.04 radians in the range of 30 ~ 80 °C. Besides, it is worth noting that errors of both amplitude and phase increase with the increase of temperature, which may be caused by the slight signal distortion.

4.3. Compensation experiment of oil film thickness

Firstly, according to the method described in Section 3.1, the acoustic speed of oil used in the experiment, as shown in Table 1, was

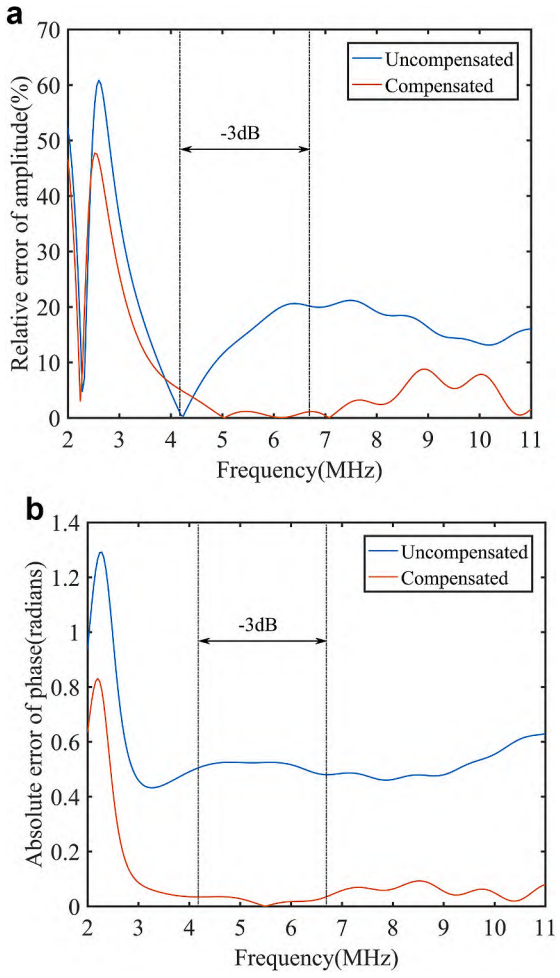

Fig. 14. The relative error of the amplitude (a) and the absolute error of the phase (b) between the compensated reference signal, the uncompensated reference signal (that is the initial reference signal), and the actual reference signal.

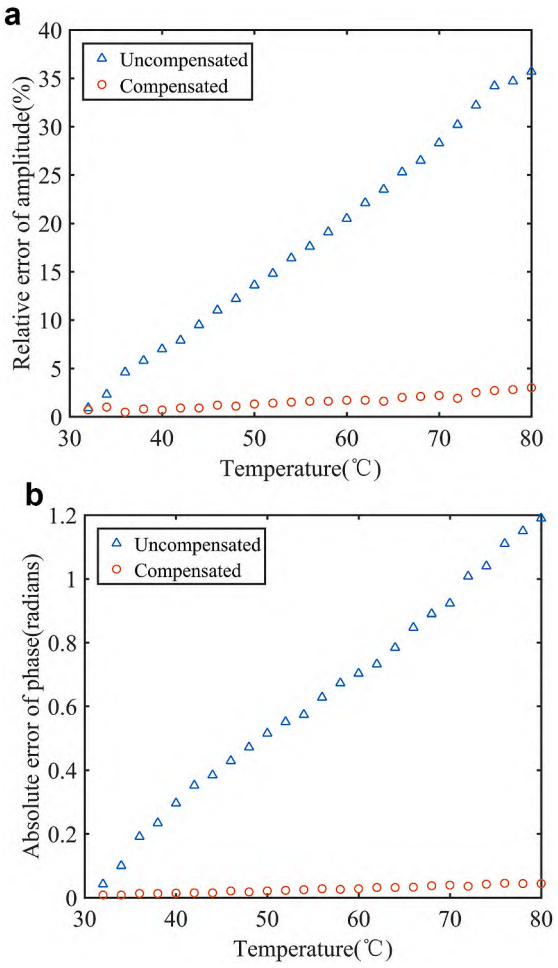

Fig. 15. The average error within -3dB bandwidth at different temperatures, (a) the amplitude error of the compensated reference signal, (b) the phase error of the compensated reference signal.

compensated. The relationship between acoustic speed c_2 and the temperature T is as follows:

$$c_2 = 1540 - 3.13T \tag{20}$$

Secondly, according to the method described in Section 3.2, the density of oil used in the experiment is compensated, and the relationship between the density ρ and the temperature T is as follows:

$$\rho = 886[1 - 0.00065(T - 20)] \tag{21}$$

Then, the positioning rig was heated in a temperature control box, and the temperature was recorded by a thermocouple. After reaching the set temperature, the temperature was kept constant. Oil was dropped onto the surface of the stationary disk, and the contact between the stationary disk and the movable disk was controlled by the micrometer. The initial film thickness was considered to be zero. By adjusting the micrometer, we can control the oil film thickness from thin to thick with a step size of 10 μm. In this process, the displacement increment of the micrometer and initial film thickness was added to construct actual oil film thicknesses. In order to verify the performance of the comprehensive temperature compensation strategy proposed in this paper for all ultrasonic models, the film thickness range is configured to cover the area from the spring model to the resonance model. The reflection signals of different thicknesses were recorded, and the reference signals were compensated according to the comprehensive compensation model in Section 3.3. The reflection coefficient amplitude spectrum was obtained by dividing the amplitude spectrum of the oil film signal and the

amplitude spectrum of the compensated reference signal. The reflection coefficient phase spectrum was obtained by subtracting the phase spectrum of the compensated reference signal and oil film signal.

The amplitude spectrum and phase spectrum of the reflection coefficient in the non-resonant region after compensating the reference signal at 45 °C are shown in Fig. 16. It can be seen that the amplitude spectrum is interlaced with each other, and the phase spectrum is obviously separated. In this region, the oil film thickness is calculated by the spring model, phase model, or complex model.

The amplitude spectrum and phase spectrum of the reflection coefficient in the resonance model region after compensating the reference signal at 45 °C are shown in Fig. 17. Obvious minimum points in the reflection coefficient amplitude spectrum and zero-crossing points in the reflection coefficient phase spectrum are observed due to the resonance behaviour. The frequencies of minimum points and zero-crossing points are extracted to calculate the film thickness by the resonance model.

The final calculated values of the oil film thickness calculated by six ultrasonic models after compensation for acoustic speed, density, and the reference signal to the actual values, and plotted in Fig. 18 (a). Resonance model-amplitude and resonance model-phase represent the results of extracting the frequency of the minimum point and zero-crossing point by Eq (8); the spring model-amplitude represent the result calculated by Eq (6); the spring model-phase is the result calculated by Eq (7); the phase model is the result calculated by Eq (2); and the complex model represents the result calculated by Eq (9). Besides, for the spring model-amplitude, spring model-phase, phase model, and the composite model, multiple frequencies within - 3 dB bandwidth are

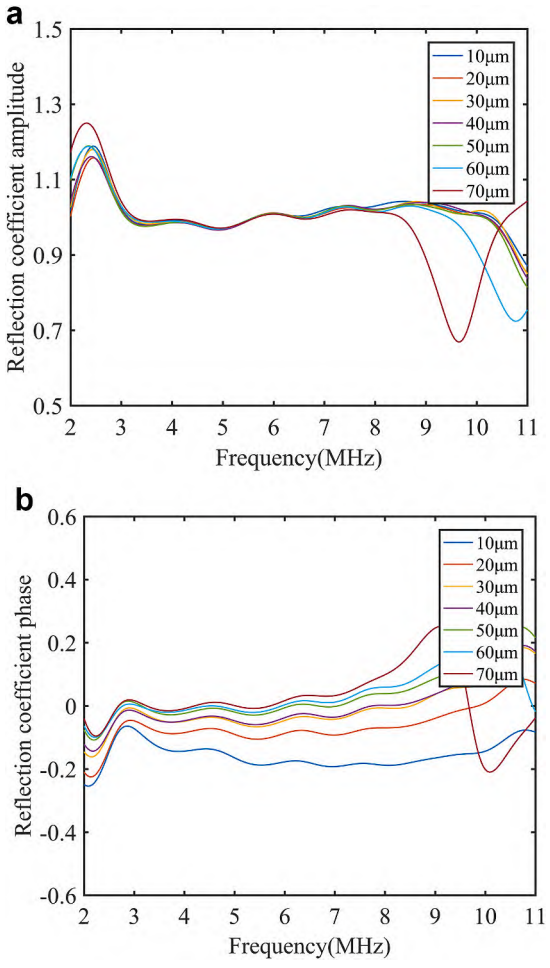

Fig. 16. The amplitude spectrum and phase spectrum of the reflection coefficient in the non-resonant region after compensating reference signal at 45 °C.

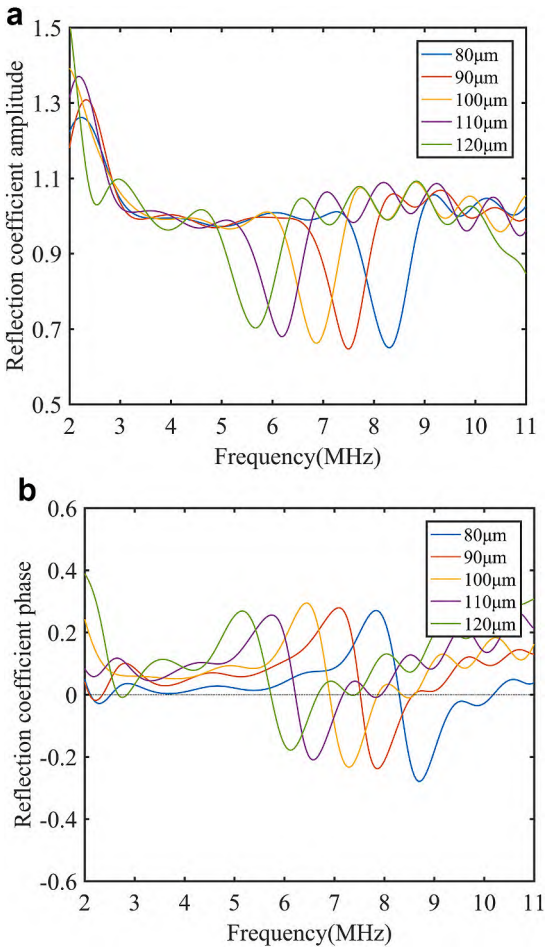

Fig. 17. The amplitude spectrum (a) and phase spectrum (b) of the reflection coefficient in the resonance region after compensating reference signal at 45 °C.

selected to calculate oil film thickness. To reduce the noise interference, the average oil film thickness is taken as the final oil film thickness. For comparison, the calculated film thickness without compensation is shown in Fig. 18 (b).

It can be observed from Fig. 18 (a) that the calculated values have a good agreement with the actual values; whereas a small error is seen when the thickness is calculated by the phase model and complex model, this is due to the considerable uncertainty of these models in the area. The results demonstrate that the temperature compensation strategy that comprehensively considers the acoustic speed, density and reference signal proposed in this paper can achieve accurate measurement of film thickness, and is applicable to all ultrasonic measurement models.

5. Conclusion

Addressing the inaccuracy of film thickness measurement with the ultrasonic principle, the effect of temperature is systematically analyzed to extract sensitive factors, thus figuring out a practical strategy. With the supports of both theoretical and experimental analysis, it can be drawn that the comprehensive temperature compensation strategy can realize the accurate measurement of oil film thickness under variable temperature conditions. The details of the benefits are:

1) The influence mechanism of temperature is clarified. On this basis, two kinds of compensation models have been figured out: a) an acoustic speed and density compensation model for material parameters, and b) a reference signal compensation model considering signal time shift, waveform expansion, and amplitude attenuation.

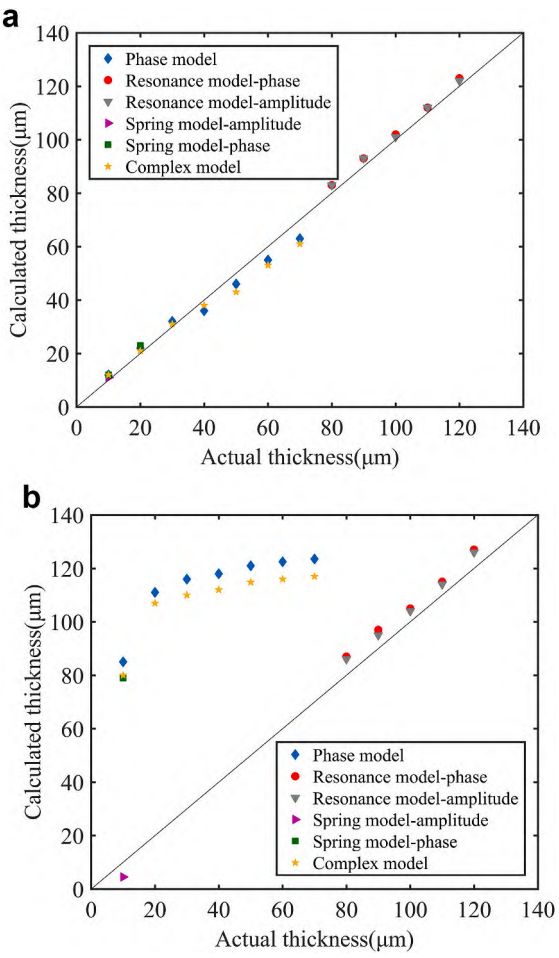

Fig. 18. (a)The comparison of the actual film thickness with oil film thickness calculated by six ultrasonic models after compensation for acoustic speed, density and the reference signal; Resonance model-amplitude and resonance model-phase represent the results of extracting the frequency of the minimum point and zero-crossing point by Eq (8), the spring model-amplitude represent the result calculated by Eq (6), the spring model-phase is the result calculated by Eq (7), the phase model is the result calculated by Eq (2), and the complex model represent the result calculated by Eq (9); (b) The comparison of the actual film thickness with oil film thickness calculated without compensation.

2) The experimental examination of the reference signal compensation indicates that the proposed model in this paper can accurately compensate for the amplitude and phase of the reference signal at the actual temperatures.
3) A comprehensive temperature compensation strategy is established and examined with experiments. The results suggest that the compensation strategy based on acoustic speed, density, and reference signal has both a good compensation effect and a wide application scope covering the zones of the spring, resonance, phase, and the complex model.

Declaration of competing interest

The authors declare that they have no known competing financial interests or personal relationships that could have appeared to influence the work reported in this paper.

Acknowledgements

The authors appreciate the financial support from the National Science Foundation of China (No. 51675403 and No. 51975455) and the support of Xi' an JingHui Information Technology Co., Ltd.

References

[1] S. Beamish, X. Li, H. Brunskill, A. Hunter, R.S. Dwyer-Joyce, Circumferential film thickness measurement in journal bearings via the ultrasonic technique, Tribol. Int. 148 (2020), https://doi.org/10.1016/j.triboint.2020.106295.
[2] L. Angrisani, A. Baccigalupi, R.S. Lo Moriello, A measurement method based on Kalman filtering for ultrasonic time-of-flight estimation, IEEE Trans. Instrum. Meas. 55 (2) (2006) 442–448, https://doi.org/10.1109/IMTC.2004.1351030.
[3] T. Reddyhoff, S. Kasolang, R.S. Dwyer-Joyce, B.W. Drinkwater, The phase shift of an ultrasonic pulse at an oil layer and determination of film thickness, Proc. Inst. Mech. Eng. Part J J. Eng. Tribol. 219 (2005), https://doi.org/10.1243/2F135065005X34044.
[4] A. Hunter, R. Dwyer-Joyce, P. Harper, Calibration and validation of ultrasonic reflection methods for thin-film measurement in tribology, Meas. Sci. Technol. 23 (2012), https://doi.org/10.1088/0957-0233/23/10/105605.
[5] J. Zhang, B.W. Drinkwater, R.S. Dwyer-Joyce, Calibration of the ultrasonic lubricant-film thickness measurement technique, Meas. Sci. Technol. 16 (2005) 1784–1791, https://doi.org/10.1088/0957-0233/16/9/010.
[6] P. Dou, T. Wu, Z. Luo, Z. Peng, T. Sarkodie-Gyan, The application of the principle of wave superposition in ultrasonic measurement of lubricant film thickness, Meas. J. Int. Meas. Confed. 137 (2019), https://doi.org/10.1016/j.measurement.2019.01.057.
[7] R.S. Dwyer-Joyce, P. Harper, B.W. Drinkwater, A method for the measurement of hydrodynamic oil films using ultrasonic reflection, Tribol. Lett. 17 (2004) 337–348, https://doi.org/10.1023/B:TRIL.0000032472.64419.1f.
[8] M. Yu, L. Shen, T. Mutasa, P. Dou, T. Wu, T. Reddyhoff, Exact analytical solution to ultrasonic interfacial reflection enabling optimal oil film thickness measurement, Tribol. Int. (2020) 106522, https://doi.org/10.1016/j.triboint.2020.106522.
[9] P. Dou, T. Wu, Z. Luo, Wide range measurement of lubricant film thickness based on ultrasonic reflection coefficient phase spectrum, J. Tribol. 141 (2019), https://doi.org/10.1115/1.4041511.
[10] G. Nicholas, T. Howard, H. Long, J. Wheals, R.S. Dwyer-Joyce, Measurement of roller load, load variation, and lubrication in a wind turbine gearbox high speed shaft bearing in the field, Tribol. Int. 148 (2020), https://doi.org/10.1016/j.triboint.2020.106322.
[11] T. Geng, Q. Meng, K. Zhang, X. Yuan, Q. Jia, Ultrasonic measurement of lubricant film thickness in sliding bearings with thin liners, Meas. Sci. Technol. 26 (2014) 25002, https://doi.org/10.1088/0957-0233/26/2/025002.
[12] R.S. Mills, R.S. Dwyer-Joyce, Ultrasound for the non-invasive measurement of IC engine piston skirt lubricant films, Proc. Inst. Mech. Eng. Part J J. Eng. Tribol. 228 (2014) 1330–1340, https://doi.org/10.1177/1350650114538616.
[13] R.S. Mills, E.Y. Avan, R.S. Dwyer-Joyce, Piezoelectric sensors to monitor lubricant film thickness at piston-cylinder contacts in a fired engine, Proc. Inst. Mech. Eng. Part J J. Eng. Tribol. 227 (2013) 100–111, https://doi.org/10.1177/1350650112464833.
[14] T. Reddyhoff, R.S. Dwyer-Joyce, P. Harper, Ultrasonic measurement of film thickness in mechanical seals, Seal. Technol. (2006) 7–11, https://doi.org/10.1016/S1350-4789(06)71260-0.
[15] T. Reddyhoff, R.S. Dwyer-Joyce, P. Harper, A new approach for the measurement of film thickness in liquid face seals, Tribol. Trans. 51 (2008) 140–149, https://doi.org/10.1080/10402000801918080.
[16] S. Kasolang, R.S. Dwyer-Joyce, Observations of film thickness profile and cavitation around a journal bearing circumference, Tribol. Trans. 51 (2008) 231–245, https://doi.org/10.1080/10402000801947717.
[17] T. Pialucha, P.C. awley, The detection of thin embedded layers using normal incidence ultrasound, Ultrasonics 32 (1994) 431–440, https://doi.org/10.1016/0041-624X(94)90062-0.
[18] R.S. Dwyer-Joyce, B.W. Drinkwater, C.J. Donohoe, The measurement of lubricant–film thickness using ultrasound, Proc. Roy. Soc. London Ser. A: Math. Phys. Eng. Sci. 459 (2003) 957–976, https://doi.org/10.1098/rspa.2002.1018.
[19] S. Kasolang, R.S. Dwyer-Joyce, M.A. Ahmad, PZT transducer design and pulsing optimization for film thickness and viscosity measurement, Sensors Actuators A Phys. 203 (2013) 386–393, https://doi.org/10.1016/j.sna.2013.08.039.
[20] P. Dou, T. Wu, Z. Peng, A time-domain ultrasonic approach for oil film thickness measurement with improved resolution and range, Meas. Sci. Technol. (2020), https://doi.org/10.1088/1361-6501/ab7a69.
[21] R. Demirli, J. Saniie, Model-based estimation of ultrasonic echoes, Part I: analysis and algorithms, IEEE Trans. Ultrason. Ferroelectrics Freq. Contr. 48 (2001) 787–802, https://doi.org/10.1109/58.920713.
[22] R. Demirli, J. Saniie, Model-based estimation of ultrasonic echoes, Part II: nondestructive evaluation applications, IEEE Trans. Ultrason. Ferroelectrics Freq. Contr. 48 (2001) 803–811, https://doi.org/10.1109/58.920714.